Original Article

MOLECULAR METABOLISM

Obesity induces resistance to central action of BMP8B through a mechanism involving the BBSome

Eva Rial-Pensado [1,2,4], Oscar Freire-Agulleiro [1,2,4], Marcos Ríos [1,2], Deng Fu Guo [3], Cristina Contreras [1,2], Patricia Seoane-Collazo [1,2], Sulay Tovar [1,2], Rubén Nogueiras [1,2], Carlos Diéguez [1,2], Kamal Rahmouni [3,], Miguel López [1,2,*]**

ABSTRACT

Objective: Bone morphogenetic protein 8B (BMP8B) plays a major role in the regulation of energy homeostasis by modulating brown adipose tissue (BAT) thermogenesis and white adipose tissue (WAT) browning. Here, we investigated whether BMP8B's role in metabolism is affected by obesity and the possible molecular mechanisms underlying that action.

Methods: Central treatments with BMP8B were performed in rats fed a standard (SD) and high-fat diet (HFD), as well as in genetically modified mice. Energy balance studies, infrared thermographic analysis of BAT and molecular analysis of the hypothalamus, BAT and WAT were carried out.

Results: We show for the first time that HFD-induced obesity elicits resistance to the central actions of BMP8B on energy balance. This obesity-induced BMP8B resistance is explained by **i)** lack of effects on AMP-activated protein kinase (AMPK) signaling, **ii)** decreased BMP receptors signaling and **iii)** reduced expression of Bardet-Biedl Syndrome 1 (BBS1) protein, a key component of the protein complex BBSome in the ventromedial nucleus of the hypothalamus (VMH). The possible mechanistic involvement of BBS1 in this process is demonstrated by lack of a central response to BMP8B in mice carrying a single missense disease-causing mutation in the *Bbs1* gene.

Conclusions: Overall, our data uncover a new mechanism of central resistance to hormonal action that may be of relevance in the pathophysiology of obesity.

Keywords Obesity; Hypothalamus; AMPK; BAT; BMP8B; BBS1

1. INTRODUCTION

Obesity results from a chronic positive energy balance due to excessive access to food and/or decreased energy expenditure, as well as genetic susceptibility and environmental factors [1—3]. Our understanding of the molecular mechanisms that mediate the control of energy balance has greatly improved over the last three decades. Despite this, the development of effective strategies to manage the current obesity pandemic has been hampered, largely due to the limited knowledge of the mechanisms underlying resistance to the action of critical metabolic hormones, such as leptin or insulin in the context of obesity [1—5].

The classical view considered that leptin resistance may develop via different mechanisms: i) impaired transport through tanycytes of the blood—brain-barrier (BBB) [6,7]; ii) deficient leptin signaling [1,6,8]; iii) counterregulatory molecular suppressors induced by leptin receptor (LepR) signaling, such as suppressors of cytokine signaling 3 (SOCS3) [9,10] and protein tyrosine phosphatase 1b (PTP1b) [11,12]; and iv) inflammation, lipotoxoticy and ER stress [13—15]. Recent evidence has also demonstrated a new mechanism that underlies leptin resistance: the impaired trafficking of LepR to the cell membrane in key hypothalamic neuronal populations. Indeed, the BBSome, a cluster of eight Bardet-Biedl Syndrome (BBS) proteins (BBS1, BBS2, BBS4, BBS5, BBS7, BBS8, BBS9 and BBS18), has emerged as a key player in the cell surface expression of key receptors mediating energy homeostasis, including the LepRb. BBSome deficiency was shown to result in inabilty of the LepRb to reach the plasma membrane, leading to leptin resistance and obesity [16—20]. This novel mechanism of

[1]Department of Physiology, CIMUS, University of Santiago de Compostela-Instituto de Investigación Sanitaria, Santiago de Compostela, 15782, Spain [2]CIBER Fisiopatología de la Obesidad y Nutrición (CIBERobn), 15706, Spain [3]Department of Neuroscience & Pharmacology, University of Iowa Carver College of Medicine, Iowa City, IA, 52242, USA

[4] Eva Rial-Pensado and Oscar Freire-Agulleiro have equally contributed to this work.

*Corresponding author. Department of Physiology, CIMUS, University of Santiago de Compostela-Instituto de Investigación Sanitaria, Santiago de Compostela, 15782, Spain. E-mail: m.lopez@usc.es (M. López).

**Corresponding author. E-mail: kamal-rahmouni@uiowa.edu (K. Rahmouni).

Received November 12, 2021 • Revision received February 14, 2022 • Accepted February 17, 2022 • Available online 23 February 2022

https://doi.org/10.1016/j.molmet.2022.101465

leptin resistance was shown to account for the obesity and leptin resistance evoked by mutations in *BBS* genes.

Bone morphogenetic protein 8B (BMP8B), a member of the transforming growth factor beta (TGFβ)-BMP superfamily, has recently emerged as a new batokine, secreted by brown/beige adipocytes [21]. Current data point to BMP8B as a major molecule in whole body metabolism by modulating **i)** brown adipose tissue (BAT) thermogenesis and the browning of white adipose tissue (WAT), through its action on AMP-activated protein kinase (AMPK) in the ventromedial nucleus of the hypothalamus (VMH) [21–23]; **ii)** the remodeling of the neurovascular network in adipose tissue acting through paracrine actions [23]; and **iii)** hepatic lipid metabolism and inflammation [24]. Notably, the relevance of BMP8B has been demonstrated in humans, and current data have also linked BMP8B to the progression of non-alcoholic steatohepatitis [24], as well as to the thermogenic response in babies [25]. Considering this evidence, the aim of this study was to investigate **i)** whether BMP8B role in metabolism is affected by obesity and **ii)** the molecular mechanisms underlying possible resistance to BMP8B actions on energy homeostasis.

2. MATERIALS AND METHODS

2.1. Animals

Adult female Sprague–Dawley rats (50–60 g; *Centro de Biomedicina Experimental; Santiago de Compostela*) and *Bbs1*$^{M390R/M390R}$ mice (University of Iowa) [26] and their littermates on a C57BL/6 background (27–30 g) were used. Animals were housed on a 12 h light (8:00–20:00) 12h dark cycle in a temperature and humidity-controlled room and maintained with chow and water *ad libitum*. Rats were divided into two main feeding groups: **i)** standard laboratory diet (SD, *SAFE A04:* 3.1% fat, 59,9% carbohydrates, 16,1% proteins, 2.791 kcal/g*; Scientific Animal Food & Engineering*; Nantes, France), and **ii)** high-fat diet (HFD, D12451: 60% fat, 20% carbohydrate, 20% protein, 5.21 kcal/g; *Research Diets, Inc*; New Brunswick, US). The animals were housed individually during 8 weeks with these diets until experimental procedures started. During all experimental procedures, animals were individually housed, and their food intake and body weight were monitored daily. The experiments were performed in agreement with the International Law on Animal Experimentation and approved by the USC Ethical Committee (Project ID 15010/14/006 and 15012/2020/010) and the University of Iowa Animal Research Committee (Protocol 8101549).

2.2. Central treatments

For chronic treatments in rats, BMP8B (0.1 pmol/day/rat; *R&D Systems*, Minneapolis, MN, USA) was delivered via a permanent 28-gauge stainless steel cannula (*Plastics One*, Roanoke, VA, USA) inserted bilaterally in the VMH, directed to the following stereotaxic coordinates: 2.8 mm posterior to bregma, ± 0.6 mm lateral to midline and 10.1 mm ventral [21,22]. A catheter tube was connected from each infusion cannula to an osmotic minipump flow moderator (Model 1007D; *Alzet Osmotic Pumps*, Cupertino, CA, USA). The osmotic minipumps were inserted in a subcutaneous pocket on the dorsal surface created using blunt dissection, and the treatment was given for 7 days. The experiment was repeated twice, resulting in 15–19 rats per group.

For chronic treatments in mice, intracerebroventricular (ICV) cannulae were stereotaxically implanted under ketamine/xylazine anesthesia as previously described [22,27] and using the following coordinates: 1.2 mm lateral to bregma, 0.6 mm posterior and 2.5 mm deep. Because of the limited number of mice available, we decided to perform ICV rather than stereotaxic administration within the VMH due to the neuroanatomical defects associated with BBS mice [26] that make it difficult to perform brain-site specific microinjections. This was also based on BMP8B actions, which are mainly mediated by the VMH and not in other hypothalamic sites such as the arcuate nucleus or lateral hypothalamic area [21,22]. After recovery, mice were treated daily with vehicle (2 μL of saline for mice) or BMP8B (2 μL of 100 pM/day/mouse; *R&D Systems*, Minneapolis, MN, USA). We used 7–8 wildtype (WT) mice and 4–5 *Bbs1*$^{M390R/M390R}$ mice per group. Since these mutant mice are naturally obese [26], they were 50% food restricted during 4 weeks before the BMP8B central treatment to avoid any confounding effect of their body weight [26]. At the start of the procedure, the animals' body weight was 40.43 ± 1.37 g. After 4 weeks on this schedule, they weighed 27.59 ± 0.73 g, in the same range as the wildtype mice (27.38 ± 0.39 g).

2.3. Temperature measurements

Skin temperature surrounding BAT was recorded with an infrared camera (B335: Compact-Infrared-Thermal-Imaging-Camera; FLIR) and analyzed with a specific software package (FLIR-Tools-Software; FLIR). In all cases, the average temperature of the selected area was chosen [22,28–31].

2.4. Sample processing

Rats and mice were killed by cervical dislocation. From each animal, we dissected the VMH and the lateral hypothalamic area (LHA) (from the whole hypothalamus, for western blot), as well as the BAT (for both western blot and mRNA analysis), the subcutaneous white adipose tissue (sWAT) and the gonadal adipose tissue (gWAT) depots (for immunohistochemistry). Each harvested tissue was immediately homogenized on ice to preserve mRNA and phosphorylated proteins. Samples were stored at −80 °C until further processing. Dissection of the VMH and the LHA was performed by micropunches under the microscope, as shown [22,28,29,32]. The specificity of the VMH dissections was confirmed by analyzing the mRNA of proopiomelanocortin (POMC), steroidogenic factor 1 (SF1) and prepro-orexin**,** as in our previous studies [22,28,29,32].

2.5. Western blotting

Protein lysates from the VMH and the LHA were subjected to SDS-PAGE, electrotransferred to polyvinylidene difluoride membranes (PVDF; *Bio-Rad;* Hercules, CA, USA) with a semidry blotter and probed with antibodies against BBS1 (1:1,000; ab166613), ALK4 (1:1,000; ab109300), ALK5 (1:1,000; ab31013), ALK7 (1:1,000; ab77051), (*Abcam;* Cambridge, UK); β-actin (1:5,000; A5316), α-tubulin (1:5,000; T5168) (*Sigma;* St Louis, MO, USA); AMPKα1 (1:1,000; 07–350), AMPKα2 (1:1,000; 07–363) (*Millipore;* Billerica, MA, USA); ACCα (1:1,000; 3662S); pAMPKα-Thr^{172} (1:1,000; 2535S); pACCα-Ser^{79} (1:1,000; 3661), CaMKK2 (1:1,000; 16810S), pLKB1 (1:1,000; 3482S), pp38 (1:1,000; 9211), pSMAD 1/5/8 (1:1,000; 13,820), TAK1 (1:250; 4505S) (*Cell Signaling*; Danvers; MA, USA); and OX-A (1:1,000; *Biossusa,* Woburn, MA, USA) [22,27,28,30–34]. Autoradiographic films (*Fujifilm*; Tokyo, Japan) were scanned, and the bands signal was quantified by densitometry using *ImageJ-1.44* software (*National Institutes of Health*; Bethesda, MD, USA) [22,27,28,30–34]. Values were expressed in relation to α-tubulin (BAT) or β-actin (VMH). Representative images for all proteins are shown, with all bands for each picture

derived from the same gel, although they may be spliced for clarity. ALK7, p38, pSMAD and BBS1 were assayed in the same membranes, therefore, some of the β-actin bands are common in their representative panels; this has been specified in Figure 5B—C and Figure 6B—C. We used 7 animals per experimental group in the VMH analyses and 13—14 animals per experimental group in the BAT analyses.

2.6. Immunohistochemistry

Adipose tissue depots were fixed in 10% buffered formaldehyde and paraffin embedded. For the hematoxylin—eosin processing, the WAT sections were first stained with hematoxylin for 5 min, washed and stained again with eosin for 1 min. Detection of UCP1 in WAT was performed using anti-UCP1 antibody (1:500; ab10983) (*Abcam*, Cambridge, UK) [27,29,31,32,35—37]. Images were taken with an Olympus XC50 digital camera (*Olympus Corporation*; Tokyo, Japan) at 20X. Digital images for WAT were quantified with *ImageJ 1.44* software (*National Institutes of Health*; Bethesda, MD, USA) [27,29,31,32,35—37]. We used 6—8 animals per experimental group.

2.7. Real-time quantitative RT-PCR

Quantitative Real-time PCR (*TaqMan®; Applied Biosystems*; Foster City, CA, USA) was performed using **i)** specific primers and probes for peroxisome-proliferator activated receptor-gamma co-activator 1 alpha (*Ppargc1a;* NM_031,347, Fw Primer 5′-CGATCACCATATTCCAGGT CAAG-3'; Rv primer 5′-CGATGTGTGCGGTGTCTGTAGT-3'; Probe FAM-5′-AGGTCCCCAGGCAGTAGATCCTCTTCAAGA-3′-TAMRA) or **ii)** commercially available validated *TaqMan®* primers and probes (*Applied Biosystems*; Foster City, CA, USA) for peroxisome-proliferator activated receptor-gamma co-activator 1 beta (PGC1β, *Ppargc1b;* Assay ID Rn_00598,552_m1), peroxisome-proliferator-activated receptor gamma (PPARγ, *Pparg;* Assay ID Rn_00440,945_m1), PR domain containing 16 (PRDM16, *Prdm16;* Assay ID Rn_01516224_m1), cell death-inducing DFFA-like effector a (CIDEA, *Cidea;* Assay ID Rn_04181355_m1), otopetrin 1 (OTOP1, *Otop1;* Assay ID Rn_00710,679) and iodothyronine deiodinase 2 (DIO2, *Dio2;* Assay ID Rn_00581,867_m1) [27,32,34]. Values were expressed in relation to hypoxanthine-guanine phosphoribosyl-transferase levels (*Hprt;* NM_012,583, FW Primer 5′-AGC CGACCGGTTCTGTCAT-3'; Fw Primer 5′-GGTCATAACCTGGTTCATCAT CAC-3'; Probe FAM-5′-CGACCCTCAGTCCCAGCGTCGTGAT-3′-TAMRA).

2.8. Statistical analysis

Data are expressed as mean ± SEM. Protein and mRNA data were expressed in relation (%) to control (vehicle-treated) animals. Error bars represent SEM. Statistical significance was determined by T test, where $P < 0.05$ was considered significant. In the energy balance plots (Figure 1G—H), data were analyzed by nonlinear regression using the extra sum-of-squares F test as a comparison method with the P values shown in the graphs that represent the global (shared) probability. Data analysis was performed using *GraphPad Instat* 3.1 and *Prism Software* 8.0.2 (*GraphPad;* San Diego, CA, US).

3. RESULTS

3.1. BMP8B in the VMH fails to induce negative energy balance in obese rats

Current evidence indicates that central BMP8B promotes BAT thermogenesis in rats and mice fed a SD [21,22]. We aimed to investigate whether the role of BMP8B on metabolism was affected by obesity. Rats fed a HFD gained significantly more weight, driven by a higher caloric intake (Figure 1A—B), confirming the efficiency of the diet-induced obesity (DIO) procedure. To investigate whether the effect of BMP8B on energy balance was dependent on the nutritional status, rats fed both a SD or a HFD were specifically treated within the VMH with BMP8B. In rats fed a SD, BMP8B injected into the VMH promoted a feeding-independent weight loss (Figure 1C—D). This response was totally absent in HFD obese rats (Figure 1E—F). Thus, the net effect of BMP8B treatment in the VMH was to induce a state of negative energy balance in SD but not HFD fed rats (Figure 1G—H). This evidence suggests that obesity induced a state of resistance to the central actions of BMP8 on energy balance.

3.2. BMP8B in the VMH fails to induce thermogenesis in obese rats

Given the feeding-independent weight loss induced by central BMP8B, we next evaluated its effect on BAT thermogenesis in lean and obese rats. Treatment with BMP8B within the VMH induced a marked elevation in the temperature of the BAT area of rats fed a SD (Figure 2A), as well as the body temperature (Figure 2B), which were associated to a significant increase in UCP1 protein levels (Figure 2C) and the expression of thermogenic markers, such as *Ppargc1a*, *Pparg* and *Otop1* in the BAT (Figure 1D). However, no changes in either BAT temperature (Figure 2E), body temperature (Figure 2F), UCP1 protein content (Figure 2G) or BAT thermogenic markers (Figure 2H) were detected in rats fed a HFD after BMP8B administration in the VMH.

3.3. BMP8B in the VMH is unable to induce browning in obese rats

Considering the effect of central BMP8B on BAT, we next evaluated its action on WAT browning. Analysis of WAT showed that central BMP8B induced a marked browning phenotype in both sWAT and gWAT depots of rats fed a SD, as demonstrated by the decreased adipocyte area (Figure 3A—B) and increased UCP1 immunostaining (Figure 3C—D). Again, no changes were found in either the sWAT or the gWAT when BMP8B was given in the VMH of HFD fed rats, in terms of the adipocyte area (Figure 3E—F) or UCP1 immunostaining (Figure 3G—H).

3.4. BMP8B in the VMH does not inhibit hypothalamic AMPK signaling in obese rats

Recent data have demonstrated that the central effects of BMP8B on BAT thermogenesis and browning are mediated by the specific inhibition of AMPK in the VMH [21,22]. We aimed to investigate whether HFD-induced obesity resulted in changes in the effect of BMP8B on AMPK in the VMH. Our data showed that while BMP8B treatment reduced the protein levels of phosphorylated AMPK (pAMPKα), and its target pACCα, in the VMH of rats fed a SD (Figure 4A), this response was absent in HFD-induced obese rats (Figure 4B). To gain further insight into the molecular mechanisms leading to the lack of effect of BMP8B on AMPK in the VMH, we explored the upstream kinases modulating AMPK activity. Our data demonstrated that in lean rats, BMP8B induced a decrease in the levels of calcium/calmodulin-dependent protein kinase kinase 2 (CaMKK2) but did not alter the phosphorylation levels of hepatic kinase B1 (LKB1) or TAK1 (also called mitogen-activated protein kinase kinase kinase 7; MAP3K7) (Figure 4C). Notably, when HFD obese rats were treated with BMP8B in the VMH, no changes were found in the protein levels of the upstream AMPK regulators (Figure 4D). Since recent data have linked orexin neurons in the LHA with the VMH AMPK-mediated stimulatory effect of BMP8B on BAT thermogenesis [22], we analyzed the hypothalamic content of OX-A. As expected, BMP8B elicited an increase in the levels of OX-A in the LHA of SD fed rats (Figure 4E), which was totally absent in HFD fed rats (Figure 4F). Overall, this evidence indicates that obesity induced a resistance to the catabolic and thermogenic actions of central BMP8B, which relates to impaired AMPK-mediated responses within the VMH, and subsequently to OX in the LHA.

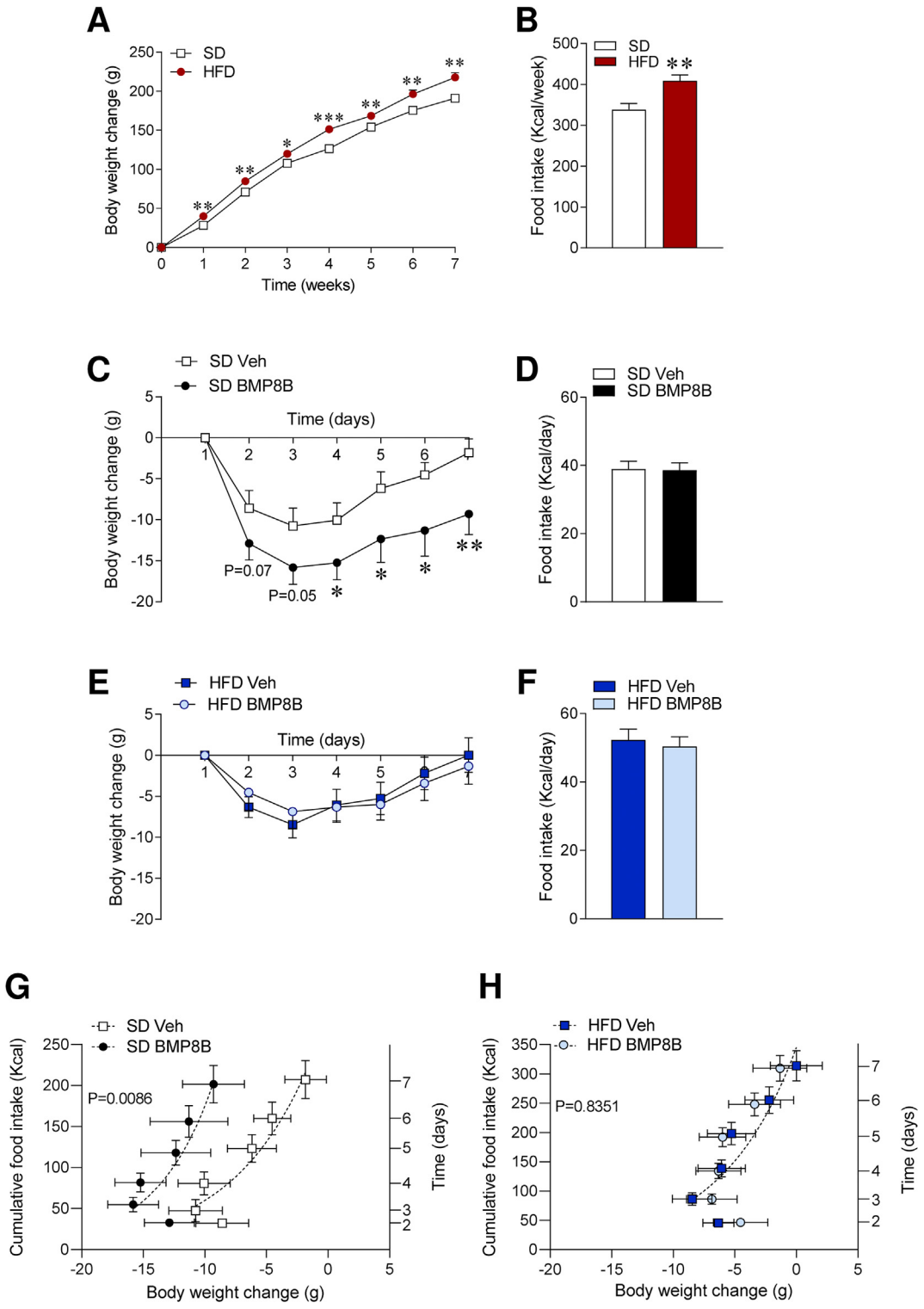

Figure 1: Effect of central BMP8B administration on energy balance in SD and HFD fed rats. (A) Body weight and **(B)** food intake of SD and HFD fed rats. **(C)** Body weight and **(D)** food intake of rats fed a SD stereotaxically injected into the VMH with vehicle or BMP8B. **(E)** Body weight and **(F)** food intake of rats fed a HFD stereotaxically injected into the VMH with vehicle or BMP8B. **(G–H)** Energy balance plots rats fed a SD **(G)** or a HFD **(H)** stereotaxically injected into the VMH with vehicle or BMP8B. Data are expressed as mean ± SEM. n = 15–19 rat/group. Statistical significance was determined by T-test (one-sided P value in the **D and H**). In **G-H**, data were analyzed by nonlinear regression using the extra sum-of-squares F test as comparison method; the P values shown in the graphs represent the global (shared) probability. *P < 0.05, **P < 0.01 *vs.* SD, SD Veh, HFD Vehicle.

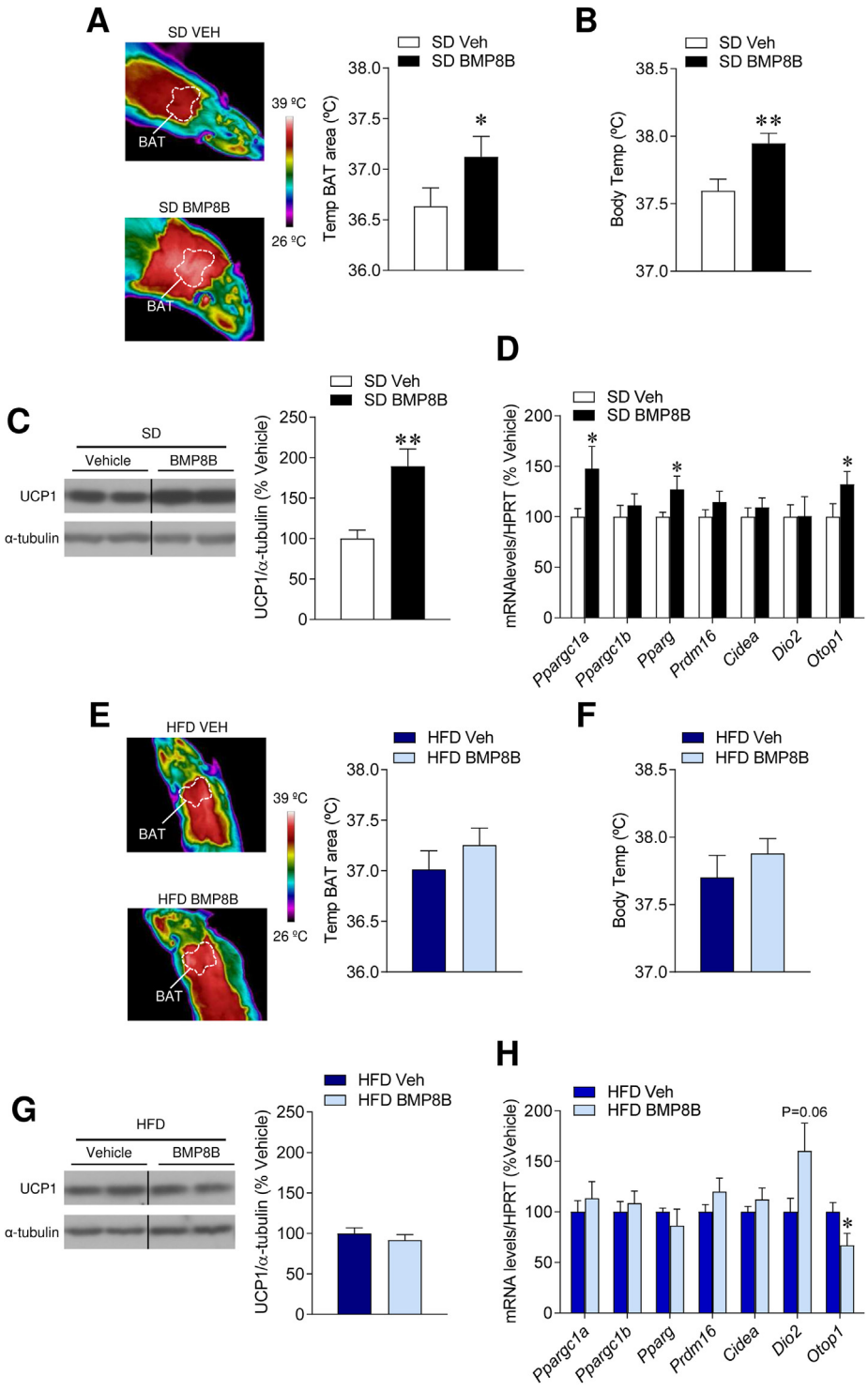

Figure 2: Effect of central BMP8B administration on BAT in SD and HFD fed rats. (A) Representative thermal images and BAT temperature, **(B)** body temperature, **(C)** western blot representative images and BAT UCP1 protein levels and **(D)** mRNA expression of thermogenic markers of rats fed a SD stereotaxically injected into the VMH with vehicle or BMP8B. **(E)** Representative thermal images and BAT temperature, **(F)** body temperature, **(G)** western blot representative images and BAT UCP1 protein levels and **(H)** mRNA expression of thermogenic markers of rats fed a HFD stereotaxically injected into the VMH with vehicle or BMP8B. In the western blot analysis, data were expressed in relation to α-tubulin (loading control). Representative images for all proteins are shown; all the bands for each picture derived from the same gel, although they may be spliced for clarity. Data are expressed as mean ± SEM. n = 15–19 rats/group for the BAT temperature analysis and n = 13–14 for the UCP1 analyses. Statistical significance was determined by T-test. *P < 0.05, **P < 0.01 *vs.* SD Vehicle.

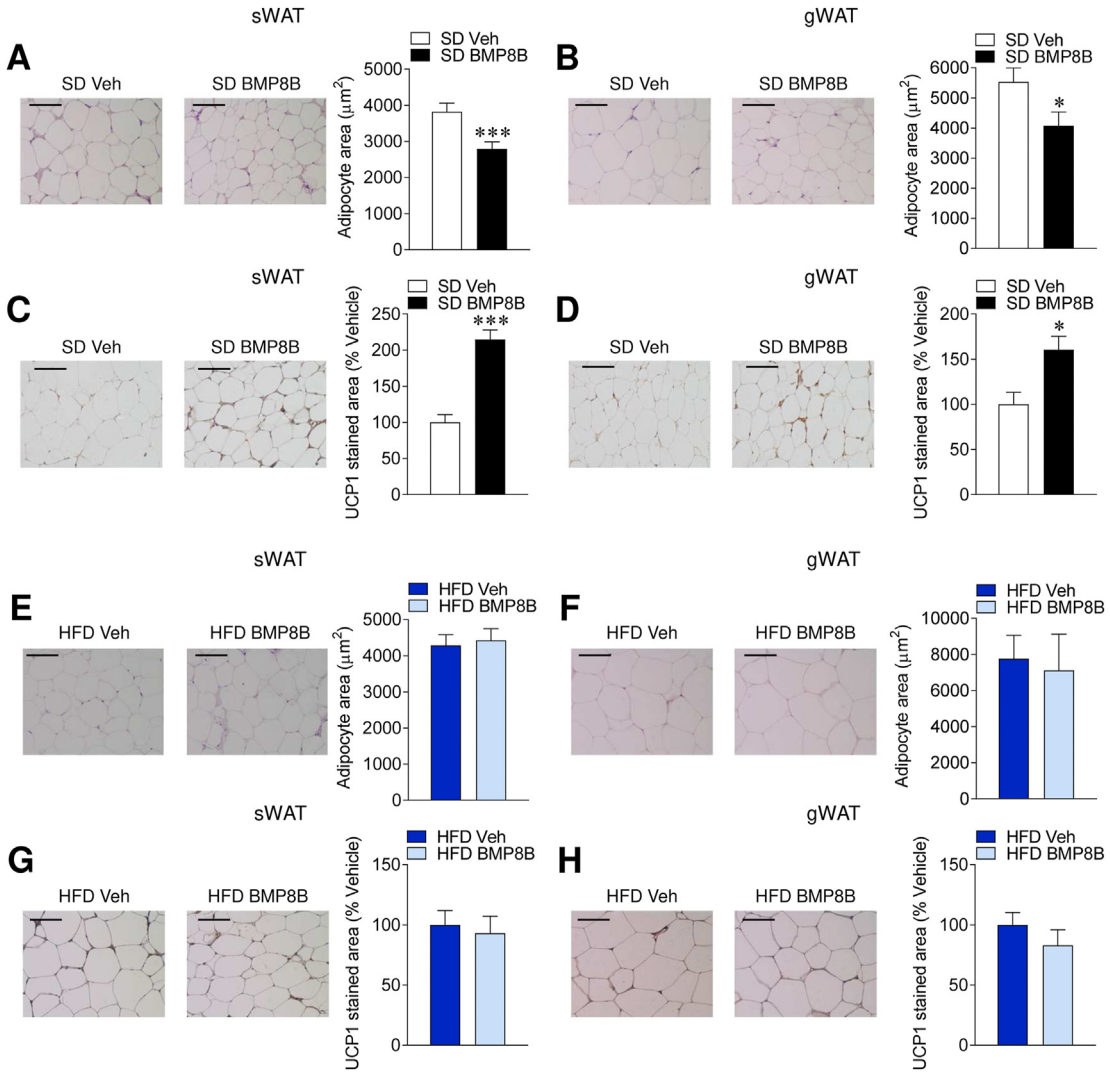

Figure 3: Effect of central BMP8B administration on browning of WAT in SD and HFD fed rats. (A—B) Representative hematoxylin-eosin staining and adipocyte area in sWAT **(A)** or gWAT **(B)** and **(C—D)** representative immunohistochemistry with anti-UCP1 antibody showing UCP1 stained area (scale bar: 100 μm) in sWAT **(C)** or gWAT **(D)** of rats fed a SD stereotaxically injected into the VMH with vehicle or BMP8B. **(E—F)** representative hematoxylin-eosin staining and adipocyte area in sWAT **(E)** or gWAT **(F)** and **(G—H)** representative immunohistochemistry with anti-UCP1 antibody showing UCP1 stained area (scale bar: 100 μm) in sWAT **(G)** or gWAT **(H)** of rats fed a HFD stereotaxically injected into the VMH with vehicle or BMP8B. Data are expressed as mean ± SEM. n = 6—8 rats/group. Statistical significance was determined by T-test. *P < 0.05, ***P < 0.001 *vs.* SD Vehicle.

3.5. BMP8B desensitizes its signaling in the VMH of obese rats

Several molecular mechanisms could explain central resistance to hormone action, including a reduction in receptor expression and/or signaling [1,8]. Therefore, we first examined the expression of BMP receptors ALK4, ALK5 and ALK7 in the VMH of HFD fed rats. Our results showed that the protein levels of these receptors were not affected by HFD (Figure 5A), indicating that a decrease in receptor levels was not responsible for the impaired BMP8B action in the hypothalamus. Next, we investigated the effect of BMP8B treatment within the VMH on the protein levels of the same receptors and downstream targets, such as phosphorylated SMAD (pSMAD) and phosphorylated p38 (pp38) [24]. While BMP8B treatment did not affect the levels of the receptors or pp38, it induced an increase in the pSMAD levels in the VMH in rats fed a SD (Figure 5B). On the other hand, BMP8B promoted a severe downregulation in the levels of ALK5, ALK7, pSMAD and pp38, but not ALK4, in rats fed a HFD (Figure 5C). Overall, these data indicate that within the context of obesity, BMP8B desensitizes its own signaling pathway in the VMH.

3.6. Lack of BBS1 function recapitulates the HFD-induced resistance to BMP8B

BBS proteins are known to play a role in the regulation of energy balance by the control of cell surface expression of key hormone receptors, such as LepR [1,16—19,38]. Thus, we hypothesized that an impaired central response to BMP8B could be mediated by changes in the BBSome. To test this, we first analyzed the protein levels of BBS1, the main BBS protein involved in energy balance [1,16—19,38]. Our data showed lower BBS1 protein levels in the VMH of rats fed a HFD (Figure 6A). Further analysis showed that central administration of BMP8B reduced BBS1 protein content in the VMH of rats fed a HFD, but not in those fed a SD (Figure 6B—C).

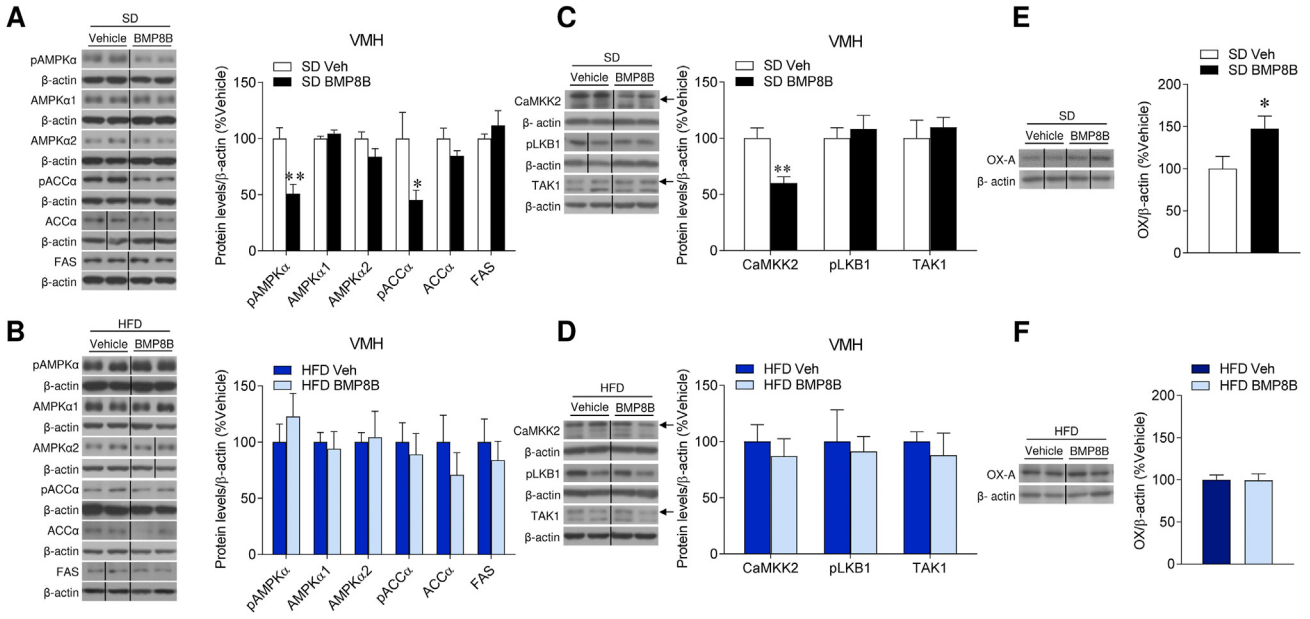

Figure 4: Effect of central BMP8B administration on AMPK pathway in the VMH and OX in LHA of SD and HFD fed rats. **(A)** Western blot images and protein levels of the AMPK pathway in the VMH, **(C)** western blot images and protein levels of the upstream AMPK kinases in the VMH and **(E)** western blot images and protein levels of OX-A in the LHA of rats fed a SD stereotaxically injected into the VMH with vehicle or BMP8B. **(B)** Western blot images and protein levels of the AMPK pathway in the VMH, **(D)** western blot images and protein levels of the upstream AMPK kinases in the VMH and **(F)** western blot images and protein levels of OX-A in the LHA of rats fed a HFD stereotaxically injected into the VMH with vehicle or BMP8B. In the western blot analyses, values were expressed in relation to β-actin. Representative images for all proteins are shown; all the bands for each picture are derived from the same gel, although they may be spliced for clarity. Data are expressed as mean ± SEM. N = 7 rats/group. Statistical significance was determined by T-test. *P < 0.05, **P < 0.01 *vs.* SD Veh, HFD Vehicle.

This evidence suggested that reduced BBS1 protein expression could be associated with central resistance to BMP8B in obesity. To directly test this idea, we treated *Bbs1*$^{M390R/M390R}$ mice and their wildtype littermates centrally with BMP8B. *Bbs1*$^{M390R/M390R}$ mice carry a single missense disease-causing mutation in the *Bbs1* gene [26]. Our data showed that whereas BMP8B induced a marked (and expected) increase in BAT temperature in wildtype mice (Figure 6D), it failed to do so in *Bbs1*$^{M390R/M390R}$ animals (Figure 6E). Overall, these data demonstrate that BBS1 plays an essential role in mediating the central effects of BBP8B on thermogenesis and energy balance.

4. DISCUSSION

The current worldwide obesity pandemic is associated with a rising incidence of morbidity and mortality due to the many medical conditions that excess fat accumulation causes [1–3]. The tendency of physiological systems to maintain homeostasis is a challenging issue, at both pathophysiological and therapeutic levels. For example, the evolutive drive to achieve positive energy balance contributes to weight aggravation in obese subjects [1–3]. On the other hand, while a vigorous hormonal biological reaction is activated to restore depleted fat stores, excess of adiposity is associated with the absence of significant response to endocrine factors. This is what is known as resistance to hormone action, and it characterizes, among other things, the impaired response to leptin or insulin in obese states [1–5]. BMP8B, a member of the TGFβ-BMP superfamily, has recently emerged as a key secreted factor regulating energy balance through endocrine and paracrine actions [21–25]. Several studies have reported that central BMP8B promotes BAT thermogenesis and WAT browning through modulation of hypothalamic AMPK [21,22]. However, the central action of BMP8B in obesity has not been studied. Here, we show that rats fed a HFD did not respond to central BMP8B administration, indicating the development of resistance to BMP8B in obesity. We demonstrate that this is due to impaired effects of BMP8B on AMPK signaling in the VMH, a key mechanism modulating thermogenesis [21,22,28,29,31–34,39], associated with reduced receptor expression/signaling and decreased BBS1 protein levels in the same nucleus. These results are of relevance for several reasons. First, they reveal a new pathophysiological mechanism for obesity: the central resistance to a batokine's action, namely BMP8B. Although central resistance to other endocrine signals, originating from the gastrointestinal tract (i.e., ghrelin and insulin) or in the WAT (i.e., leptin) is well-known, the central resistance to BAT-secreted factors [40,41] remains unclear. It has been shown, for example, that the peripheral response to fibroblast growth factor 21 (FGF21, which is produced by BAT, besides from the liver) [42] is impaired in obesity, but no data have shown impaired central responses. Second, these results corroborate that the mechanisms underlying central BMP8B resistance are common to those described for other hormones, such as leptin and insulin. Third, the findings shed new light about the role of BBS proteins on energy balance [1–5].

BMP8B signaling is complex and different from the canonical BMPs downstream events. Whereas most BMPs signal via either the branch of the SMAD pathway involving ALK receptor tyrosine kinase (ALK) proteins ALK4, ALK5 and ALK7 (signaling via SMAD2/3) or through ALK1, ALK2, ALK3 and ALK6 (signaling via SMAD1/5/8(9)), BMP8B signals via both [21,23,24,43–45]. The exact neuronal population where the desensitization of BMP8B takes place remains obscure; however, considering that the effects of VMH AMPK as a canonical modulator of thermogenesis, are located in SF1 neurons [29,32,34], it is tempting to speculate that impaired BMP8B signaling occurs in this neuronal population. Further work, in particular with neuronal-specific mouse models

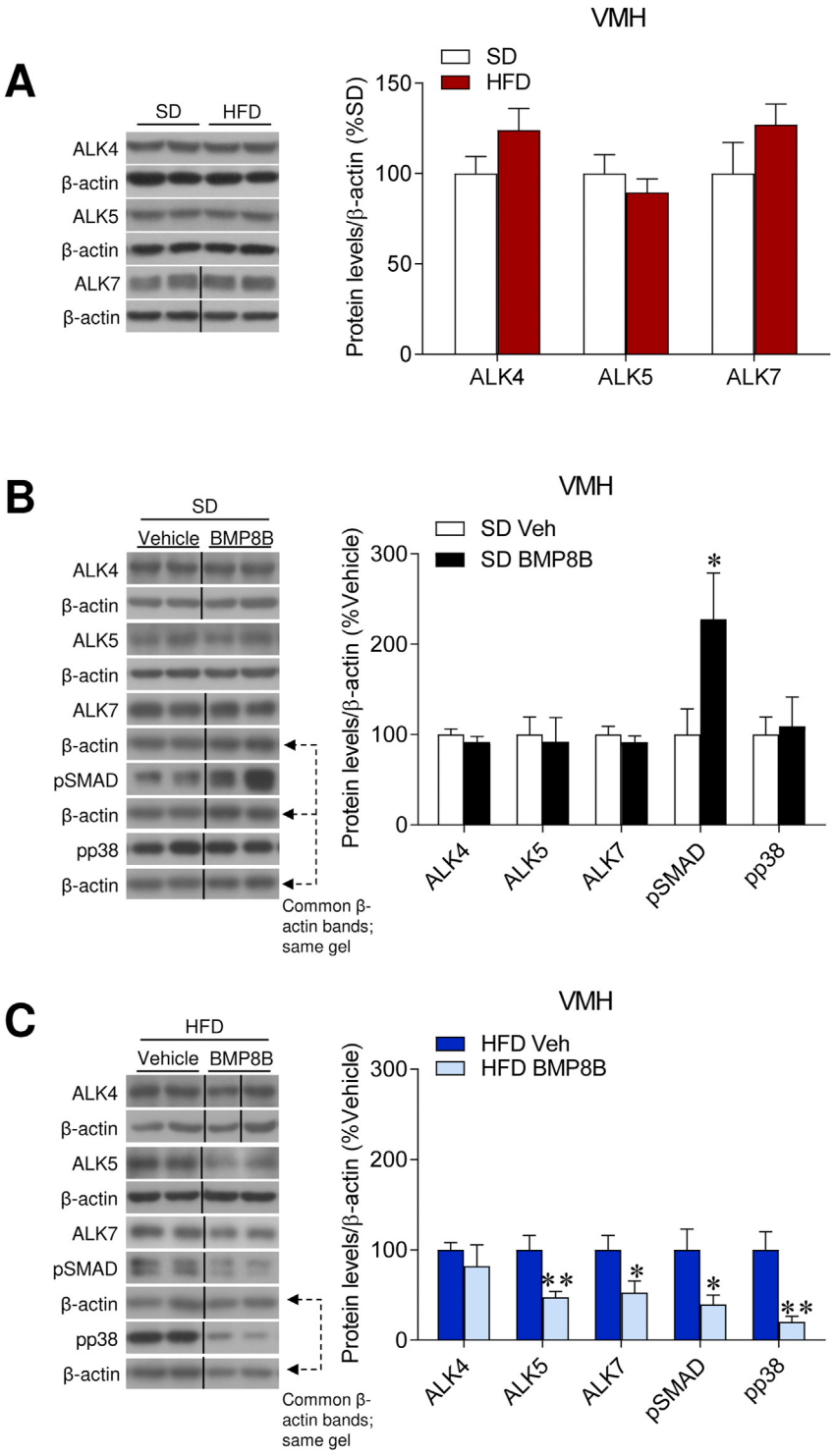

Figure 5: Effect of central BMP8B administration on BMP Type I receptors signaling in the VMH of SD and HFD fed rats. (A) Western blot images and protein levels of the BMP receptors in the VMH of SD and HFD fed rats. **(B)** Western blot images and protein levels of the BMP receptors in the VMH of rats fed a SD stereotaxically injected into the VMH with vehicle or BMP8B fed a SD. **(C)** Western blot images and protein levels of the BMP receptors in the VMH of rats fed a HFD stereotaxically injected into the VMH with vehicle or BMP8B. In the western blot analyses, values were expressed in relation to β-actin. Representative images for all proteins are shown; all the bands for each picture are derived from the same gel, although they may be spliced for clarity. ALK7, pp38, pSMAD and BBS1 were assayed in the same membranes, therefore, some of the β-actin bands are common in their representative panels; this has been specified in Figure 5B–C and Figure 6B–C. Data are expressed as mean ± SEM. N = 7 rats/group. Statistical significance was determined by T-test. *P < 0.05, **P < 0.01 *vs.* SD, SD Vehicle.

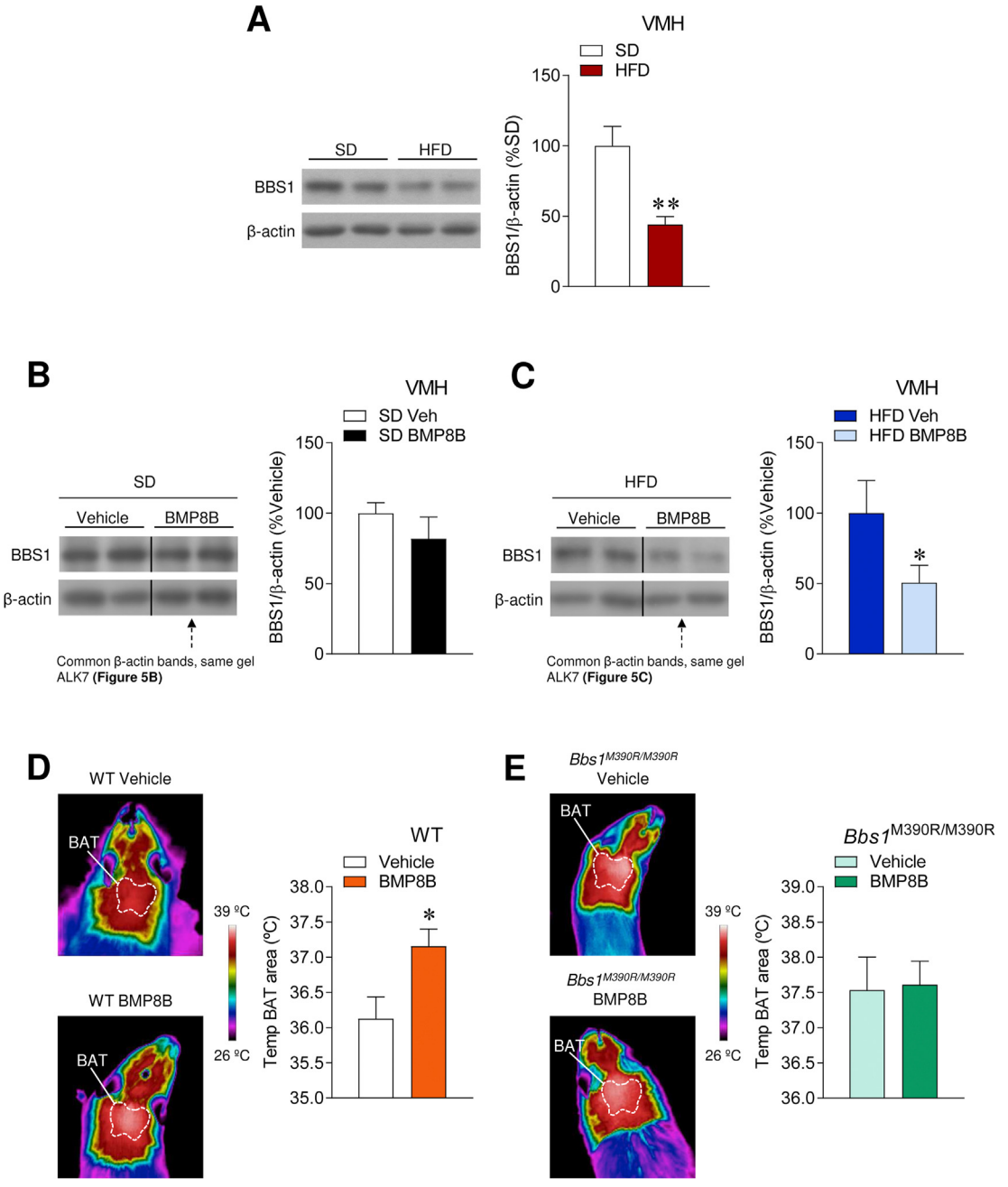

Figure 6: Effect of ICV administration of BMP8B in *Bbs1*$^{M390R/M390R}$ mice. **(A)** Western blot images and protein levels of BBS1 in the VMH of SD and HFD fed rats. **(B)** Western blot images and protein levels of BBS1 in the VMH of rats fed a SD stereotaxically injected into the VMH with vehicle or BMP8B. **(C)** Western blot images and protein levels of BBS1 in the VMH of rats fed a HFD stereotaxically injected into the VMH with vehicle or BMP8B. **(D)** BAT temperature and representative thermal images of WT mice ICV treated with vehicle or BMP8B. **(E)** BAT temperature and representative thermal images of *Bbs1*$^{M390R/M390R}$ mice ICV treated with vehicle or BMP8B. In the western blot analyses, values were expressed in relation to β-actin. Representative images for all proteins are shown; all the bands for each picture are derived from the same gel, although they may be spliced for clarity. ALK7, pp38, pSMAD and BBS1 were assayed in the same membranes, therefore, some of the β-actin bands are common in their representative panels; this has been specified in Figure 5B–C and Figure 6B–C. Data are expressed ad mean ± SEM. n = 7 rats/group **(A–C)** and n = 4–8 mice/group (7–8 WT and 4–5 *Bbs1*$^{M390R/M390R}$; **D-E**). Statistical significance was determined by T-test. *P < 0.05, **P < 0.01 *vs.* SD, HFD Vehicle, WT Vehicle.

such as the SF1 BBS1 KO mice, that we have recently generated and reported [19], will be needed to address this issue.

Our data also implicate the BBSome to be associated with the central resistance to BMP8B. BBSome deficiency evoked by loss of *BBS* genes lead to obesity in human and animal models [16,20,38,46]. This obese phenotype of BBS is driven by neuronal mechanisms, as indicated by the observation that mice lacking the *Bbs1* gene in the nervous system, but not adipose tissue, develop obesity [20]. Moreover, targeted deletion of the *Bbs1* gene in key populations of hypothalamic neurons (such as SF1, POMC and agouti-related protein, AgRP) also causes obesity in mice [17–19]. Interestingly, the obesity induced by *Bbs1* gene deletion in SF1 neurons of the VMH was due to the reduction in

BAT thermogenesis with no significant change in food intake [19]. Mechanistically, we have showed that BBS-associated obesity is caused by the reduction in the sensitivity to various hormones that govern energy homeostasis due to a decrease in the surface expression of their receptors. This includes the LepRb and 5-HT_{2C} receptors. In the present study, we extend these findings by demonstrating that the BBSome is a critical determinant of neuronal BMB8B sensitivity. This is supported by the reduced BBS1 protein levels in the VMH of obese rats and after BMP8B administration. The fact that resistance to central BMP8B is recapitulated in *Bbs1*$^{M390R/M390R}$ mice demonstrates that BBSome deficiency evoked by reduction in BBS1 levels/function is associated with resistance to BMP8B. Although the exact molecular mechanisms underlying this effect will require further investigation, this could relate to a reduction in ALK receptors trafficking to the plasma membrane; this, in addition to their decreased expression (ALK5 and ALK7), may be responsible of the observed reduced signaling. This possibility is supported by the reduced pSMAD and pp38 protein levels in obese rats after BMP8B treatment. Alternatively, a reduction in BBSome function in the VMH, specifically in SF1 neurons, could lead to diminished LepR trafficking and then to leptin resistance, like mice lacking the *Bbs1* gene in those neurons [19]. Supporting this idea is the fact that the AMPK—SNS—BAT axis is modulated by leptin [47]. A third possibility is that both effects may take place, and resistance to BMP8B is the result of a synergistic action, due to loss of both BMP8B and leptin signaling.

5. CONCLUSIONS

In summary, this study demonstrates that obesity induces resistance to central BMP8B actions on energy homeostasis and uncovers a possible functional connection between its receptor signaling pathway, AMPK and BBSome. Further work involving BBS1 overexpression in specific neuronal populations in the context of obesity, as well as the SF1 BBS1 KO mice that we have recently generated and reported [19], will shed new light about the mechanistic link between BMP8B and the BBSome. Considering the recently discovered involvement of BMP8B in the regulation of metabolism in humans [24,25], this evidence suggests that resistance to BMP8B could be a pathological mechanism of common human obesity.

AUTHOR'S CONTRIBUTIONS

ER-P, OF-A, CC and PS-C performed the in vivo experiments, analytical methods collected and analyzed the data.
DFG and KR provided the Bbs1M390R/M390R mice.
ER-P, OF-A, MR, DFG, RN, CD, KR and ML analyzed, interpreted and discussed the data.
KR and ML developed the hypothesis and conceived and designed the experiments.
ML made the figures and wrote the manuscript.
All authors revised and edited the manuscript.
ML is the lead contact of this study, supervised this work, secured funding and coordinated the project.

ACKNOWLEDGEMENTS

The research leading to these results received funding from the Xunta de Galicia (RN: 2016-PG057); Ministerio de Ciencia e Innovación co-funded by the FEDER Program of EU (CD: BFU2017-87721; RN: BFU2015-70664R; ML: RTI2018—101840-B-I00); USA National Institutes of Health (KR: HL084207); the USA Department of Veterans Affairs (KR: I01BX004249); The University of Iowa Fraternal Order of Eagles Diabetes Research Center (KR); European Research Council (ERC Synergy Grant-2019-WATCH- 810331); Atresmedia Corporación (RN and ML: 2017-P0004) and "la Caixa" Foundation (ID 100010434) under agreement LCF/PR/HR19/52160022 (ML). CiMUS is supported by the Xunta de Galicia (2016—2019, ED431G/05).OF-A is recipeint of a fellowship of Xunta de Galicia (ED481A-2019/026). PS-C is recipient of a fellowship the European Union's Horizon 2020 research and innovation program under the Marie Sklodowska-Curie actions. CIBER de Fisiopatología de la Obesidad y Nutrición is an initiative of ISCIII. The funders had no role in study design, data collection and analysis, decision to publish or preparation of the manuscript.

CONFLICT OF INTEREST

Authors declare no conflict of interest.

REFERENCES

[1] Cui, H., López, M., Rahmouni, K., 2017. The cellular and molecular bases of leptin and ghrelin resistance in obesity. Nature Reviews Endocrinology 13(6):338—351.
[2] Muller, T.D., Clemmensen, C., Finan, B., Dimarchi, R.D., Tschop, M.H., 2018. Anti-obesity therapy: from rainbow pills to polyagonists. Pharmacological Reviews 70(4):712—746.
3 Dragano, N.R.V., Ferno, J., Dieguez, C., Lopez, M., Milbank, E., 2020 Jun 15. Recent updates on obesity treatments: available drugs and future directions. Neuroscience 437:215—239. https://doi.org/10.1016/j.neuroscience.2020.04.034.
[4] Friedman, J.M., 2019. Leptin and the endocrine control of energy balance. Nat Metab 1(8):754—764.
[5] White, M.F., Kahn, C.R., 2021. Insulin action at a molecular level - 100 years of progress. Molecular Metabolism 52:101304.
[6] López, M., Tovar, S., Vázquez, M.J., Nogueiras, R., Seoane, L.M., García, M., et al., 2007. Perinatal overfeeding in rats results in increased levels of plasma leptin but unchanged cerebrospinal leptin in adulthood. International Journal of Obesity 31(2):371—377.
[7] Duquenne, M., Folgueira, C., Bourouh, C., Millet, M., Silva, A., Clasadonte, J., et al., 2021. Leptin brain entry via a tanycytic LepR-EGFR shuttle controls lipid metabolism and pancreas function. Nat Metab 3(8):1071—1090.
[8] López, M., Seoane, L.M., Tovar, S., García, M.C., Nogueiras, R., Diéguez, C., et al., 2005. A possible role of neuropeptide Y, agouti-related protein and leptin receptor isoforms in hypothalamic programming by perinatal feeding in the rat. Diabetologia 48(1):140—148.
[9] Mori, H., Hanada, R., Hanada, T., Aki, D., Mashima, R., Nishinakamura, H., et al., 2004. Socs3 deficiency in the brain elevates leptin sensitivity and confers resistance to diet-induced obesity. Natura Med 10(7):739—743.
[10] Reed, A.S., Unger, E.K., Olofsson, L.E., Piper, M.L., Myers Jr., M.G., Xu, A.W., 2010. Functional role of suppressor of cytokine signaling 3 upregulation in hypothalamic leptin resistance and long-term energy homeostasis. Diabetes 59(4):894—906.
[11] Cheng, A., Uetani, N., Simoncic, P.D., Chaubey, V.P., Lee-Loy, A., McGlade, C.J., et al., 2002. Attenuation of leptin action and regulation of obesity by protein tyrosine phosphatase 1B. Developmental Cell 2(4):497—503.
[12] Bence, K.K., Delibegovic, M., Xue, B., Gorgun, C.Z., Hotamisligil, G.S., Neel, B.G., et al., 2006. Neuronal PTP1B regulates body weight, adiposity and leptin action. Natura Med 12(8):917—924.
[13] Zhang, X., Zhang, G., Zhang, H., Karin, M., Bai, H., Cai, D., 2008. Hypothalamic IKKbeta/NF-kappaB and ER stress link overnutrition to energy imbalance and obesity. Cell 135(1):61—73.
[14] Contreras, C., González-García, I., Martínez-Sánchez, N., Seoane-Collazo, P., Jacas, J., Morgan, D.A., et al., 2014. Central ceramide-induced hypothalamic lipotoxicity and ER stress regulate energy balance. Cell Reports 9(1):366—377.
[15] Liu, J., Lee, J., Salazar Hernandez, M.A., Mazitschek, R., Ozcan, U., 2015. Treatment of obesity with celastrol. Cell 161(5):999—1011.

[16] Guo, D.F., Rahmouni, K., 2011. Molecular basis of the obesity associated with Bardet-Biedl syndrome. Trends in Endocrinology and Metabolism 22(7):286—293.
[17] Guo, D.F., Cui, H., Zhang, Q., Morgan, D.A., Thedens, D.R., Nishimura, D., et al., 2016. The BBSome controls energy homeostasis by mediating the transport of the leptin receptor to the plasma membrane. PLoS Genetics 12(2):e1005890.
[18] Guo, D.F., Lin, Z., Wu, Y., Searby, C., Thedens, D.R., Richerson, G.B., et al., 2019. The BBSome in POMC and AgRP neurons is necessary for body weight regulation and sorting of metabolic receptors. Diabetes 68(8):1591—1603.
[19] Rouabhi, M., Guo, D.F., Morgan, D.A., Zhu, Z., Lopez, M., Zingman, L., et al., 2021. BBSome ablation in SF1 neurons causes obesity without comorbidities. Molecular Metabolism 48:101211.
[20] Guo, D.F., Reho, J.J., Morgan, D.A., Rahmouni, K., 2020. Cardiovascular regulation by the neuronal BBSome. Hypertension 75(4):1082—1090.
[21] Whittle, A.J., S, C., L, M., Slawik, M., Hondares, E., Vázquez, M.J., et al., 2012. Bmp8b increases brown adipose tissue thermogenesis through both central and peripheral actions. Cell 149(4):871—885.
[22] Martins, L., Seoane-Collazo, P., Contreras, C., Gonzalez-Garcia, I., Martinez-Sanchez, N., Gonzalez, F., et al., 2016. A functional link between AMPK and orexin mediates the effect of BMP8B on energy balance. Cell Reports 16(8):2231—2242.
[23] Pellegrinelli, V., Peirce, V.J., Howard, L., Virtue, S., Turei, D., Senzacqua, M., et al., 2018. Adipocyte-secreted BMP8b mediates adrenergic-induced remodeling of the neuro-vascular network in adipose tissue. Nature Communications 9(1):4974.
[24] Vacca, M., Leslie, J., Virtue, S., Lam, B.Y.H., Govaere, O., Tiniakos, D., et al., 2020. Bone morphogenetic protein 8B promotes the progression of non-alcoholic steatohepatitis. Nat Metab 2(6):514—531.
[25] Urisarri, A., Gonzalez-Garcia, I., Estevez-Salguero, A., Pata, M.P., Milbank, E., Lopez, N., et al., 2021. BMP8 and activated brown adipose tissue in human newborns. Nature Communications 12(1):5274.
[26] Davis, R.E., Swiderski, R.E., Rahmouni, K., Nishimura, D.Y., Mullins, R.F., Agassandian, K., et al., 2007. A knockin mouse model of the Bardet-Biedl syndrome 1 M390R mutation has cilia defects, ventriculomegaly, retinopathy, and obesity. Proceedings of the National Academy of Sciences of the United States of America 104(49):19422—19427.
[27] Seoane-Collazo, P., Linares-Pose, L., Rial-Pensado, E., Romero-Pico, A., Moreno-Navarrete, J.M., Martinez-Sanchez, N., et al., 2019. Central nicotine induces browning through hypothalamic kappa opioid receptor. Nature Communications 10(1):4037.
[28] Martínez de Morentin, P.B., Gónzalez-García, I., Martins, L., Lage, R., Fernández-Mallo, D., Martínez-Sánchez, N., et al., 2014. Estradiol regulates brown adipose tissue thermogenesis via hypothalamic AMPK. Cell Metabolism 20(1):41—53.
[29] Seoane-Collazo, P., Roa, J., Rial-Pensado, E., Linares-Pose, L., Beiroa, D., Ruiz-Pino, F., et al., 2018. SF1-Specific AMPKalpha1 deletion protects against diet-induced obesity. Diabetes 67(11):2213—2226.
[30] Gonzalez-Garcia, I., Contreras, C., Estevez-Salguero, A., Ruiz-Pino, F., Colsh, B., Pensado, I., et al., 2018. Estradiol regulates energy balance by ameliorating hypothalamic ceramide-induced ER stress. Cell Reports 25(2):413—423.
[31] Seoane-Collazo, P., Rial-Pensado, E., Estevez-Salguero, A., Milbank, E., Garcia-Caballero, L., Rios, M., et al., 2021. Activation of hypothalamic AMPK ameliorates metabolic complications of experimental arthritis. Arthritis & Rheumatology 74(2):212—222.
[32] Milbank, E., Dragano, N.R.V., Gonzalez-Garcia, I., Garcia, M.R., Rivas-Limeres, V., Perdomo, L., et al., 2021. Small extracellular vesicle-mediated targeting of hypothalamic AMPKalpha1 corrects obesity through BAT activation. Nat Metab 3(10):1415—1431.
[33] López, M., Varela, L., Vázquez, M.J., Rodríguez-Cuenca, S., González, C.R., Velagapudi, V.R., et al., 2010. Hypothalamic AMPK and fatty acid metabolism mediate thyroid regulation of energy balance. Natura Med 16(9):1001—1008.
[34] Martínez-Sánchez, N., Seoane-Collazo, P., Contreras, C., Varela, L., Villarroya, J., Rial-Pensado, E., et al., 2017. Hypothalamic AMPK-ER stress-JNK1 axis mediates the central actions of thyroid hormones on energy balance. Cell Metabolism 26(1):212—229.
[35] Contreras, C., Gonzalez-Garcia, I., Seoane-Collazo, P., Martinez-Sanchez, N., Linares-Pose, L., Rial-Pensado, E., et al., 2017. Reduction of hypothalamic endoplasmic reticulum stress activates browning of white fat and ameliorates obesity. Diabetes 66(1):87—99.
[36] Martinez-Sanchez, N., Moreno-Navarrete, J.M., Contreras, C., Rial-Pensado, E., Ferno, J., Nogueiras, R., et al., 2017. Thyroid hormones induce browning of white fat. Journal of Endocrinology 232(2):351—362.
[37] Fraga, A., Rial-Pensado, E., Nogueiras, R., Ferno, J., Dieguez, C., Gutierrez, E., et al., 2021. Activity-based anorexia induces browning of adipose tissue independent of hypothalamic AMPK. Frontiers in Endocrinology 12:669980.
[38] Lopez, M., 2016. Hypothalamic leptin resistance: from BBB to BBSome. PLoS Genetics 12(5):e1005980.
[39] López, M., Nogueiras, R., Tena-Sempere, M., Dieguez, C., 2016. Hypothalamic AMPK: a canonical regulator of whole-body energy balance. Nature Reviews Endocrinology 12(7):421—432.
[40] Villarroya, F., Cereijo, R., Villarroya, J., Giralt, M., 2017. Brown adipose tissue as a secretory organ. Nature Reviews Endocrinology 13(1):26—35.
[41] Villarroya, J., Cereijo, R., Gavalda-Navarro, A., Peyrou, M., Giralt, M., Villarroya, F., 2019. New insights into the secretory functions of brown adipose tissue. Journal of Endocrinology 243(2):R19—R27.
[42] Fisher, F.M., Chui, P.C., Antonellis, P.J., Bina, H.A., Kharitonenkov, A., Flier, J.S., et al., 2010. Obesity is a fibroblast growth factor 21 (FGF21)-resistant state. Diabetes 59(11):2781—2789.
[43] Tang, Y., Yang, X., Friesel, R.E., Vary, C.P., Liaw, L., 2011. Mechanisms of TGF-beta-induced differentiation in human vascular smooth muscle cells. Journal of Vascular Research 48(6):485—494.
[44] Wu, F.J., Lin, T.Y., Sung, L.Y., Chang, W.F., Wu, P.C., Luo, C.W., 2017. BMP8A sustains spermatogenesis by activating both SMAD1/5/8 and SMAD2/3 in spermatogonia. Science Signaling 10(477).
[45] Sanchez-Duffhues, G., Williams, E., Goumans, M.J., Heldin, C.H., Ten Dijke, P., 2020. Bone morphogenetic protein receptors: structure, function and targeting by selective small molecule kinase inhibitors. Bone 138:115472.
[46] Novas, R., Cardenas-Rodriguez, M., Irigoin, F., Badano, J.L., 2015. Bardet-Biedl syndrome: is it only cilia dysfunction? FEBS Letters 589(22):3479—3491.
[47] Tanida, M., Yamamoto, N., Shibamoto, T., Rahmouni, K., 2013. Involvement of hypothalamic AMP-activated protein kinase in leptin-induced sympathetic nerve activation. PLoS One 8(2):e56660.

